we have not conducted a study of **4**, the calculations on **1** and **3** suggest an alternative explanation. The more electron-withdrawing isocyanide ligand lowers the energy of the metal $d\pi$ orbitals, thereby decreasing the metal character and correspondingly increasing the sulfur character in the iron-sulfur π-antibonding HOMO ($\pi^*_{\parallel}$). This would tend to favor S-S bond formation to give the dimeric product **4**.

Another reaction of interest is the cycloaddition of electron-deficient alkynes to **1** to give a five-member heterometallacycle:[18]

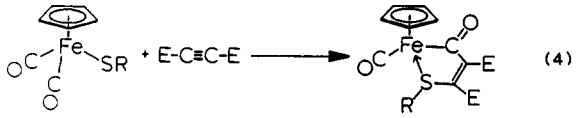

(4)

This reaction is interesting in that the addition of the alkyne takes place at two different types of ligands, a π acceptor (carbonyl) and a π donor (thiolate). The mechanism of this novel $[4\pi + 2\pi]$ cycloaddition reaction has been previously discussed.[18f]

Conclusions

Fenske-Hall molecular orbital calculations on **1** (R = H) predict a $d\pi$-$p\pi$ orbital interaction between the formally occupied $d\pi$ iron orbitals and the lone pair on sulfur that is principally 3p in character. This interaction results in a destabilized antibonding combination that is the highest occupied molecular orbital and principally sulfur 3p in character. The results of the calculations are supported by spectroscopic studies including photoelectron spectra for **1** (R = C_6H_4-*p*-Z; Z = OMe, H, Cl, CF_3, NO_2) which reveal an energetically isolated high-energy band that shows a significant substituent effect. These spectroscopic results correlate with the kinetic results obtained from the reaction of **1** and alkyl halides. Mechanistic studies of this reaction support an S_N2-type nucleophilic displacement of the halide by the coordinated thiolate ligand. The correlation of the spectroscopic and kinetic results lends additional support to our postulate that the HOMO of **1** is principally sulfur in character. We conclude that the enhanced nucleophilicity of the sulfur atom of **1** is due to a destabilizing filled-filled $d\pi$-$p\pi$ orbital interaction between the p-type sulfur lone pair and the formally occupied metal $d\pi$ orbitals. These results contrast with the stabilizing filled-empty $d\pi$-$p\pi$ orbital interactions observed for $CpMo(NO)(SR)_2$.[4d]

Acknowledgment. We wish to thank Dr. K. Christensen for assistance with the NMR experiments, Dr. G. E. Kellogg for assistance with the PES experiments carried out in the Laboratory for Electron Spectroscopy and Surface Analysis, and Prof. R. S. Glass for valuable discussion. Financial support of this work by the National Institute of Environmental Health Sciences (Grant ES 00966) (J.H.E.), the Department of Energy (Division of Chemical Sciences, Office of Basic Energy Sciences, Office of Energy Research, Grant DE-AC02-80ER10746) (D.L.L.), and the Materials Characterization Program, Department of Chemistry, University of Arizona, is gratefully acknowledged. In addition, M.T.A. thanks the University of Arizona Summer Research Support Program for their award of a research assistantship.

Registry No. **1** (R = C_6H_4-*p*-OMe), 110935-19-8; **1** (R = C_6H_5), 12110-44-0; **1** (R = C_6H_4-*p*-Cl), 110935-20-1; **1** (R = C_6H_4-*p*-CF_3), 110935-21-2; **1** (R = C_6H_4-*p*-NO_2), 110935-22-3; **1** (R = C_2H_5), 12108-34-8; **1** (R = H), 110935-18-7; **2** (R = C_2H_5, R' = $(CH_2)_4CH{=}CH_2$, X = I), 110935-23-4; **2** (R = C_6H_4-*p*-OMe, R' = Me, X = I), 110935-24-5; **2** (R = C_6H_5, R' = Me, X = I), 110935-25-6; **2** (R = C_6H_4-*p*-Cl, R' = Me, X = I), 110935-26-7; **2** (R = C_6H_4-*p*-CF_3, R' = Me, X = I), 110935-27-8; **2** (R = C_6H_4-*p*-NO_2, R' = Me, X = I), 110935-28-9; **3** (R = H), 110935-29-0; HSC_6H_4-*p*-OMe, 696-63-9; HSC_6H_5, 108-98-5; HSC_6H_4-*p*-Cl, 106-54-7; HSC_6H_4-*p*-CF_3, 825-83-2; HSC_6H_4-*p*-NO_2, 1849-36-1; $CpFe(CO)_2I$, 12078-28-3; $HS(CH_2)_4CH{=}CH_2$, 18922-04-8; 6-iodo-1-hexene, 2695-47-8; 6-(ethylthio)-1-hexene, 75199-72-3.

Notes

Contribution from the Department of Chemistry,
University of California at Santa Barbara,
Santa Barbara, California 93106

Oxygen Transfer from *p*-Cyano-*N*,*N*-dimethylaniline *N*-Oxide to the μ-Oxo Dimer of (*meso*-Tetraphenylporphinato)iron(III)

C. Michael Dicken, P. N. Balasubramanian,
and Thomas C. Bruice*

Received June 22, 1987

Dealkylation of tertiary amines in hepatic microsomes is carried out on reaction with the $NADH/O_2$ cytochrome P-450 enzymes and via flavin mixed-function oxidase conversion of the primary amine to an *N*-oxide, which then reacts with a cytochrome P-450 enzyme in a reaction that does not require NADH nor O_2.[1,2] The mechanisms of reaction of *N*-oxides with iron(III) porphyrins is of considerable interest.[3-9] In this investigation we examine the reaction of the μ-oxo dimer of (*meso*-tetraphenylporphinato)iron(III) ($((TPP)Fe^{III})_2O$) with *p*-cyano-*N*,*N*-dimethylaniline *N*-oxide (DAO). Our objectives have been to probe the reactions that proceed from the immediate higher valent product of oxygen transfer to the μ-oxo dimer (i.e., $(TPP)Fe^{III}$-O-$Fe^{IV}(O)(TPP^{\cdot+})$).

Methods and Materials

The μ-oxo dimer of (*meso*-tetraphenylporphinato)iron(III) ($((TPP)Fe^{III})_2O$) was synthesized by the method of Kobayashi and co-workers[10] and characterized by its UV-vis spectra. ***p*-Cyano-*N*,*N*-dimethylaniline *N*-oxide** (DAO) was prepared as given elsewhere.[11] The sources of all other chemicals used in this study have been reported.[5]

Results

In this investigation, the reaction of *p*-cyano-*N*,*N*-dimethylaniline *N*-oxide (DAO) with the μ-oxo dimer of (*meso*-tetraphenylporphinato)iron(III) ($((TPP)Fe^{III})_2O$) has been studied in grade A[5] CH_2Cl_2 solvent (at 25 °C under N_2). The products of decomposition of DAO are *p*-cyano-*N*,*N*-dimethylaniline (DA), *p*-cyano-*N*-methylaniline (MA), *p*-cyanoaniline (A), *p*-cyano-*N*-formyl-*N*-methylaniline (FA), *N*,*N*'-dimethyl-*N*,*N*'-bis(*p*-cyanophenyl)hydrazine (H), and *N*,*N*'-bis(*p*-cyanophenyl)-*N*-methylmethylenediamine (MD). Products with time were monitored at 320 nm, where absorption by the metalloporphyrin is minimal. Yields by HPLC analysis at 280 and 320 nm (based upon $[DAO]_i$): DA, 59%; MA, 18%; A, 3%; FA, 6%; H, 8%; MD, 7%; all at $[DAO]_i/[((TPP)Fe^{III})_2O]_i$ ratios of 10-100. The yield of

(1) White, R. E.; Coon, M. J. *Annu. Rev. Biochem.* **1980**, *49*, 315.
(2) Hamill, S.; Cooper, D. Y. *Xenobiotica* **1984**, *14*, 139.
(3) Shannon, P.; Bruice, T. C. *J. Am. Chem. Soc.* **1981**, *103*, 4580.
(4) Nee, M. W.; Bruice, T. C. *J. Am. Chem. Soc.* **1982**, *104*, 6123.
(5) Dicken, C. M.; Lu, F.-L.; Nee, M. W.; Bruice, T. C. *J. Am. Chem. Soc.* **1985**, *107*, 5776.
(6) Dicken, C. M.; Woon, T. C.; Bruice, T. C. *J. Am. Chem. Soc.* **1986**, *108*, 1636.
(7) Woon, T. C.; Dicken, C. M.; Bruice, T. C. *J. Am. Chem. Soc.* **1986**, *108*, 7990.
(8) Bruice, T. C.; Dicken, C. M.; Balasubramanian, P. N.; Woon, T. C.; Lu, F.-L. *J. Am. Chem. Soc.* **1987**, *109*, 3436.
(9) Ostovic, D.; Knobler, C. B.; Bruice, T. C. *J. Am. Chem. Soc.* **1987**, *109*, 3444.
(10) Kobayashi, H.; Higuchi, T.; Kaizu, Y.; Osada, H.; Aoki, M. *Bull. Chem. Soc. Jpn.* **1975**, *48*, 3137.
(11) Craig, J. C.; Purushothman, K. K. *J. Org. Chem.* **1970**, *35*, 1721.

0020-1669/88/1327-0197$01.50/0

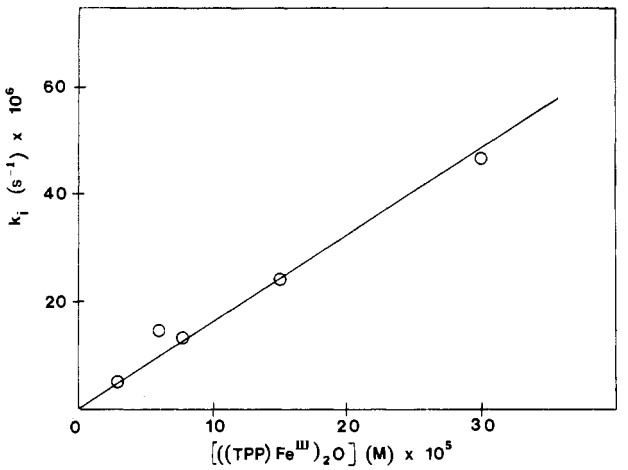

Figure 1. Plot of the first-order rate constants (k_i, determined from the initial lag phase of the kinetic traces) vs the concentration of ((TPP)-Fe^{III})$_2$O at constant $[DAO]_i$ (3.0×10^{-3} M).

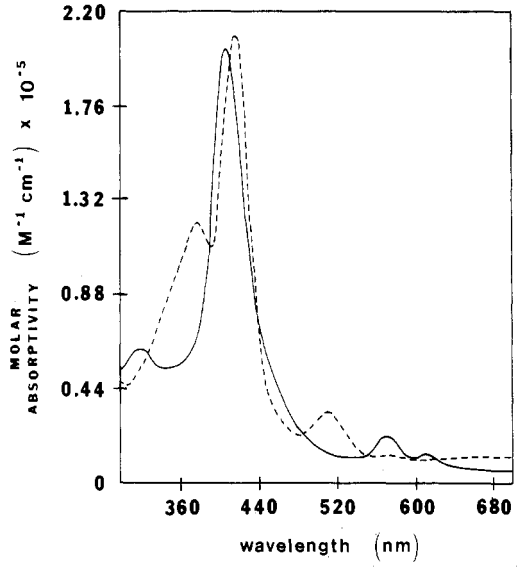

Figure 2. Visible absorption spectra of ((TPP)Fe^{III})$_2$O (1.0×10^{-4} M) in CH_2Cl_2. Spectrum A (solid line) for ((TPP)Fe^{III})$_2$O is taken prior to addition of DAO (2.70×10^{-3} M) whereas spectrum B (dashed line) corresponds to the spectrum at completion of reaction. The latter spectrum is superimposable on that of (TPP)Fe^{III}(Cl).

CH_2O based on the method of Nash[12] is 15%. Though complete material balance is obtained in N, approximately 20% of the oxygen equivalents based on $[DAO]_i$ are unaccounted for. Under the pseudo-first-order conditions of $[DAO]_i > [((TPP)Fe^{III})_2O]_i$ and at constant porphyrin concentration, the change in absorbance at 320 nm is characterized by a lag phase followed by a fractional order increase. Initial rate constants were calculated from tangential slopes drawn to the lag phases at early times by use of eq 1 (R = slope of the tangential lines, k_i = rate constant (s^{-1}),

$$k_i = R/(\epsilon_{max}[DAO]L) \quad (1)$$

ϵ_{max} = extinction coefficient calculated from $\delta A_{320}/[DAO]_i$, and L = 1 mm). Values of k_i are linearly dependent on $[((TPP)-Fe^{III})_2O]_i$ (Figure 1). Thus, the initial reaction is first order in $[((TPP)Fe^{III})_2O]$, and since k_i is independent of the $[DAO]_i$, eq 2 is established. A value of $k = k_i/[((TPP)Fe^{III})_2O] = 0.15$ M^{-1} s^{-1} is obtained from the slope of Figure 1.

$$d[P]/dt = k[((TPP)Fe^{III})_2O][DAO]$$
$$k_i = k[((TPP)Fe^{III})_2O] \quad (2)$$

(12) Nash, T. *Biochem. J.* **1953**, *55*, 416.

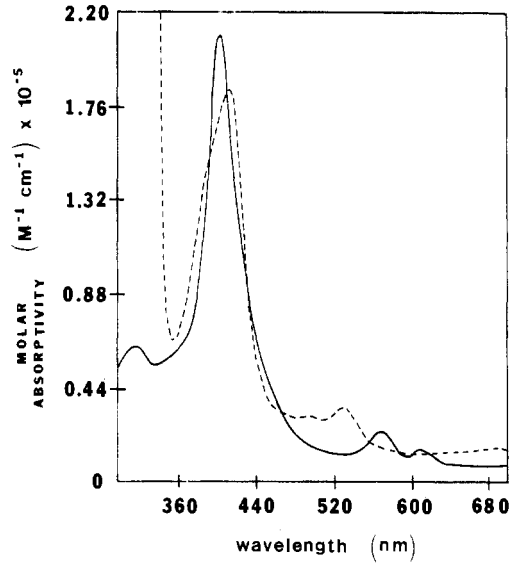

Figure 3. Visible absorption spectra of ((TPP)Fe^{III})$_2$O (2.0×10^{-4} M) in the absence (spectrum A, solid line) and presence of a large excess of PO (0.1 M, spectrum B, dashed line).

Table I. Effect of 2,3-Dimethyl-2-butene (TME) on the Kinetics and Product Yields in the ((TPP)Fe^{III})$_2$O (1.0×10^{-4} M) Catalyzed Decomposition of DAO (3.0×10^{-3} M)

	% yields of products						
$[TME]_i$, M	DA	MA	A	FA	H	MD	TMEO
0.0	59	18	3	6	8	7	0.0
0.01	63	17	2	4	5	4	31
0.10	89	4	1	1	1	1	80
1.00	93	3	0	0	0	0	94

Examination of the final visible spectrum shows that porphyrin destruction does not occur but conversion to (TPP)Fe^{III}(Cl) does. At turnover numbers >30 the final spectrum is that of (TPP)-Fe^{III}(Cl) (Figure 2). Formation of (TPP)Fe^{III}(Cl) does not occur when a solution of 1.0×10^{-4} M ((TPP)Fe^{III})$_2$O in CH_2Cl_2 solvent is stored for a time period greater than the reaction time.

Equilibrium constants for the addition of an *N*-oxide to ((TP-P)Fe^{III})$_2$O were approximated by a known procedure.[13] For this purpose picoline *N*-oxide (PO) was employed, since it has been shown to be incapable of transferring an oxygen to iron(III) porphyrins.[5] The equilibrium binding of PO was followed by monitoring the disappearance of the α,β-absorbance band (570 nm) of ((TPP)Fe^{III})$_2$O. The approximated equilibrium constants K_1 and β_2 of eq 3 were calculated to be 500 M^{-1} and 1.8×10^4 M^{-2}, respectively. Bisligation of *N*-oxide with ((TPP)Fe^{III})$_2$O may actually represent fragmentation of the structure. Thus, when an excess of PO is added to ((TPP)Fe^{III})$_2$O in CH_2Cl_2, the resulting spectrum (Figure 3) resembles that determined[14] for $[(TPP)Fe^{III}(PO)_2]^+Cl^-$.

$$((TPP)Fe^{III})_2O + PO \overset{K_1}{\rightleftharpoons} (TPP)(PO)Fe^{III}\text{–}O\text{–}Fe^{III}(TPP) \quad (3a)$$

$$((TPP)Fe^{III})_2O + 2PO \overset{\beta_2}{\rightleftharpoons} \text{“}((TPP)Fe^{III})_2O{\cdot}2PO\text{”} \quad (3b)$$

Product Formation. The time course for the formation of amine products is shown in Figure 4. The addition of 2,3-dimethyl-2-butene (TME) as a substrate has very little effect on the kinetics of the reaction. The second-order rate constants that could be calculated from the initial rates under these conditions are 0.10 M^{-1} s^{-1} (0.01 M TME), 0.21 M^{-1} s^{-1} (0.1 M TME), and 0.14 M^{-1} s^{-1} (1.0 M TME). However, the product ratios are, as is to be

(13) Walker, F. A.; Lo, M.-W.; Ree, M. T. *J. Am. Chem. Soc.* **1976**, *98*, 5552.
(14) Dicken, C. M.; Bruice, T. C., unpublished results, 1987.

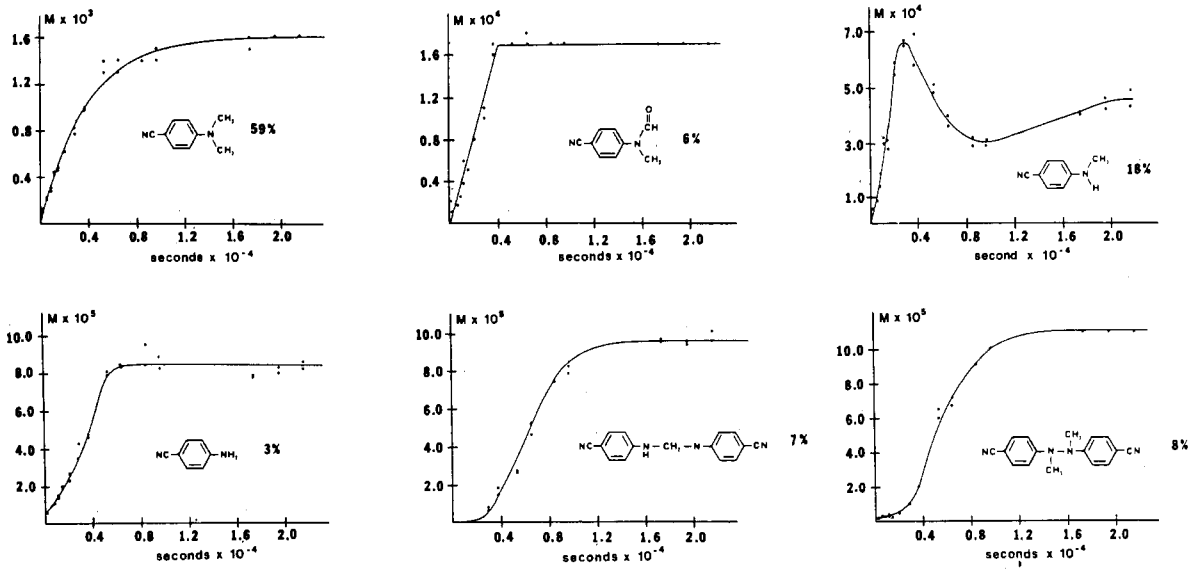

Figure 4. Plots of the time courses (determined by HPLC) for the formation of the products DA, MA, FA, A, MD, and H obtained on reaction of $((TPP)Fe^{III})_2O$ (1.0×10^{-4} M) with DAO (2.70×10^{-3} M).

expected, dependent on $[TME]_i$ (see Table I). The higher $[TME]_i$, the higher the yield of epoxide (TMEO) and DA. Thus, at increasing concentrations of TME the yields of MA, A, FA, H, and MD decrease. With 0.10 and 1.0 M TME the porphyrin exists as $((TPP)Fe^{III})_2O$ at t_∞, while at 0.01 M TME a mixture of $((TPP)Fe^{III})_2O$ and $(TPP)Fe^{III}(Cl)$ species is obtained on completion of the reaction.

Discussion

Reactions of DAO with $((TPP)Fe^{III})_2O$ exhibit a lag phase in the formation of DA at 320 nm. The correlation for the appearance of DA may be approximated to the first-order rate law. The lag phase observed by following the change in A_{320} with time was not seen when the appearance of DA was followed by HPLC. This is due to the difficulty in analysis at early times by HPLC. The correlation line for the formation of MA reveals the latter to be initially an intermediate in a consecutive two-step process and subsequently to be a final product of the oxidation. The early formation of FA with time is zero order, while at longer times the concentration of FA is invariant with time. The correlation line for the formation of A shows a slight lag phase followed by an accelerated buildup. The formation of both H and MD is characterized by pronounced lag phases followed by their first-order formation. The lag phases seen with A and particularly with H and MD are to be anticipated in that they are products of a cascade of oxidations.

Chloride ion required for the conversion $((TPP)Fe^{III})_2O \rightarrow (TPP)Fe^{III}(Cl)$ at turnover numbers >30 arises by solvent oxidation. Solvent oxidation accounts for a portion of the 20% oxygen imbalance in the reaction. Only the initial lag phase of the reaction is due solely to catalysis by $((TPP)Fe^{III})_2O$. It is difficult to determine the $(TPP)Fe^{III}(Cl)/((TPP)Fe^{III})_2O$ molar ratios as a function of reaction time. However, kinetic analysis by use of initial rates (lag phase) may be employed to determine the kinetics for reaction with $((TPP)Fe^{III})_2O$. The pseudo-first-order rate constants calculated from initial slopes show a linear dependence on the concentration of $((TPP)Fe^{III})_2O$ and independence of the initial concentration of DAO and TME.[5] These results establish that the rate-limiting step is the transfer of oxygen from DAO to $((TPP)Fe^{III})_2O$, yielding the reactive iron–oxo species, which oxidizes the substrates (S) in a rapid step (eq 4). The second-order rate constant, calculated from initial slopes, for $((TPP)Fe^{III})_2O$ (0.15 M^{-1} s^{-1}) may be compared to that of (5 M^{-1} s^{-1}) for $(TPP)Fe^{III}(Cl)$.[5] Thus, $(TPP)Fe^{III}(Cl)$ reacts with DAO nearly 35-fold faster than does $((TPP)Fe^{III})_2O$. Competition of $((TPP)Fe^{III})_2O$ and $(TPP)Fe^{III}(Cl)$ for DAO and the appreciable difference in the rate constants for the two reactions explain the fractional order for the reaction following the initial lag phase.

$$((TPP)Fe^{III})_2O + DAO \xrightarrow{k_{rds}} \text{hypervalent iron–oxo} + DA \quad (4a)$$

$$\text{hypervalent iron–oxo} + S \xrightarrow{k_{rapid}} ((TPP)Fe^{III})_2O + \text{oxidized substrates} \quad (4b)$$

Approximation of binding constants for PO ligation to $((TPP)Fe^{III})_2O$ shows that bisligation occurs (eq 3). The K_1 value ($\sim$500 M^{-1}) for monoligation to generate $((TPP)Fe^{III})_2O(PO)$ is much greater than that for the formation of $(TPP)Fe^{III}(PO)$ ($\sim$20 M^{-1}) even when the statistical advantage of the former is taken into account. The sequence of reactions in (5) may be

$$(TPP)Fe^{III}\text{–O–}Fe^{III}(TPP)(DAO) \rightarrow (TPP)Fe^{III}\text{–O–}Fe^{IV}(TPP^{\bullet+})(O) + DA \quad (5a)$$

$$(TPP)Fe^{III}\text{-O-}Fe^{IV}(TPP^{\bullet+})(O) + DA \rightarrow (TPP)Fe^{III}\text{–O–}Fe^{IV}(TPP)(OH) + DA^{\bullet} \quad (5b)$$

considered for the initial reaction steps. However, it is known that electrochemical 2e oxidation of the porphyrin μ-oxo dimer provides $((^{\bullet+}Porph)Fe^{III})_2O$.[15-17] This suggests the alternate mechanism (6) for the initial rate of oxidation. It should be noted

$$(TPP)Fe^{III}\text{–O–}Fe^{IV}(TPP^{\bullet+})(O) \rightarrow 2(TPP)Fe^{IV}(O) \quad (6a)$$

$$(TPP)Fe^{IV}(O) + DA \rightarrow (TPP)Fe^{III}(OH) + DA^{\bullet} \quad (6b)$$

$$(TPP)Fe^{IV}(O) + DA^{\bullet} \rightarrow (TPP)Fe^{III}(OH) + CA1 \quad (6c)$$

$$2(TPP)Fe^{III}(OH) \rightarrow (TPP)Fe^{III}\text{–O–}Fe^{III}(TPP) + H_2O \quad (6d)$$

that the cascade of oxidation products [DA → CA1 → MA → MA• → A; CA1 → FA; MA• → H; MA• → MD (CA1 is carbinolamine 1; see ref 5 for more details)] obtained in this study has been obtained previously with DAO plus $(TPP)Fe^{III}(Cl)$.[5] The other cascade products could be generated by one-electron oxidation of the various intermediate amine products by $(TPP)Fe^{IV}(O)$ (eq 6) and by $(^{+\bullet}TPP)Fe^{IV}(O)$ formed from the reaction of DAO with $(TPP)Fe^{III}(Cl)$.

The sequence of reactions (7) provides a plausible explanation for the conversion of $((TPP)Fe^{III})_2O$ to $(TPP)Fe^{III}(Cl)$, which

(15) Phillippi, M. A.; Goff, H. M. *J. Am. Chem. Soc.* **1982**, *104*, 6026.
(16) Phillippi, M. A.; Goff, H. M. *J. Am. Chem. Soc.* **1979**, *101*, 7641.
(17) Chang, D.; Cocolios, P.; Wu, Y. T.; Kadish, K. M. *Inorg. Chem.* **1984**, *23*, 1629.

$$(TPP)Fe^{III}\text{–}O\text{–}Fe^{IV}(TPP^{\bullet+})(O) + CH_2Cl_2 \rightarrow (TPP)Fe^{III}\text{–}O\text{–}Fe^{IV}(TPP)(OH) + {}^{\bullet}CHCl_2 \quad (7a)$$

$$(TPP)Fe^{III}\text{–}O\text{–}Fe^{IV}(TPP)(OH) + {}^{\bullet}CHCl_2 \rightarrow ((TPP)Fe^{III})_2O + HC(O)Cl + HCl \quad (7b)$$

$$(TPP)Fe^{III}\text{–}O\text{–}Fe^{IV}(TPP^{\bullet+})(O) + HC(O)Cl \rightarrow ((TPP)Fe^{III})_2O + CO_2 + HCl \quad (7c)$$

$$((TPP)Fe^{III})_2O + HCl \rightarrow (TPP)Fe^{III}OH + (TPP)Fe^{III}(Cl) \quad (7d)$$

accompanies solvent oxidation and the formation of Cl^- ions. Carbon dioxide has been identified as an oxidation product of CH_2Cl_2 in the reaction of C_6H_5IO with Ni(II) macrocycles in CH_2Cl_2.[18] Monomerization of $((TPP)Fe^{III})_2O$ may also occur on its reaction with DAO (eq 8). It has been observed that the

$$((TPP)Fe^{III})_2O + DAO \rightarrow (TPP)Fe^{III}\text{–}O\text{–}Fe^{III}(DAO)(TPP) \quad (8a)$$

$$(TPP)Fe^{III}\text{–}O\text{–}Fe^{III}(DAO)(TPP) \rightarrow (TPP)Fe^{III}(O^-) + (TPP)Fe^{III}(DAO) \quad (8b)$$

$$(TPP)Fe^{III}(DAO) + DAO \rightarrow (TPP)Fe^{III}(DAO)_2^- \quad (8c)$$

addition of a large excess of PO to $((TPP)Fe^{III})_2O$ results in the appearance of the characteristic spectrum[14] of $(TPP)Fe^{III}(PO)_2^-$.

Addition of TME to the reaction mixture of $((TPP)Fe^{III})_2O$ and DAO provides TME-epoxide as the product along with other oxidized amine products. The second-order rate constants determined from the initial rates remain reasonably constant at various concentrations of TME (0.01–1.0 M), showing that TME epoxidation is not rate-limiting. As expected, the distribution of the various products changes with respect to $[TME]_i$ (Table I) since DA etc. compete with TME for oxidation. When the concentration of TME is increased to 1.0 M, the yields of DA and TME-epoxide reach 94% and $((TPP)Fe^{III})_2O$ remains, spectrally, intact during the course of the reaction. This establishes that when there is a large excess of TME, the hypervalent iron–oxo porphyrin species is trapped totally to provide 100% yields of DA and TME-epoxide and that under such a condition solvent is not oxidized and there is no formation of $(TPP)Fe^{III}(Cl)$.

The epoxidizing species could be $(^{+\bullet}TPP)Fe^{IV}(O)\text{–}O\text{–}Fe^{III}(TPP)$ (eq 9), $(TPP)Fe^{IV}(O^-)\text{–}O\text{–}Fe^{IV}(TPP)$ (eq 10), or $(^{+\bullet}TPP)Fe^{IV}(O)$ (eq 11). To account for the initial rates in the presence of high

$$((TPP)Fe^{III})_2O + DAO \rightarrow (^{+\bullet}TPP)Fe^{IV}(O)\text{–}O\text{–}Fe^{III}(TPP) \quad (9)$$

$$(^{+\bullet}TPP)Fe^{IV}(O)\text{–}O\text{–}Fe^{III}(TPP) \rightarrow (TPP)Fe^{IV}(O^-)\text{–}O\text{–}Fe^{IV}(TPP) \quad (10)$$

$$(^{+\bullet}TPP)Fe^{IV}(O)\text{–}O\text{–}Fe^{III}(TPP) \rightarrow (TPP)Fe^{III}(O^-) + (^{+\bullet}TPP)Fe^{IV}(O) \quad (11)$$

$[TME]_i$ the initial epoxidant trapped by TME must be $(^{+\bullet}TPP)Fe^{IV}(O)\text{–}O\text{–}Fe^{III}(TPP)$. After the initial lag phase the epoxidant is reasonably $(^{+\bullet}TPP)Fe^{IV}(O)$, which after oxygen transfer to substrate is complete, reconverts to the $((TPP)Fe^{III})_2O$ state. The $(TPP)Fe^{IV}(O^-)\text{–}O\text{–}Fe^{IV}(TPP)$ species is likely to be unimportant as an epoxidant. Thus, at low temperatures iron(IV)–oxo porphyrin shows no reactivity with alkenes.[19]

Acknowledgment. This work was supported by the National Institutes of Health.

Registry No. DAO, 62820-00-2; TME, 563-79-1; $((TPP)Fe^{III})_2O$, 12582-61-5.

(18) Koola, J. D.; Kochi, J. K. *Inorg. Chem.* **1987**, *26*, 916.
(19) (a) Mansuy, D. *Pure Appl. Chem.* **1987**, *59*, 759. (b) Balch, A. L., private communication.

Contribution from the Department of Chemistry, University of Colorado at Colorado Springs, Colorado Springs, Colorado 80933-7150

Synthesis, Characterization, and Solvatochromic Studies of Group 6 Metal Carbonyls Bound to the Bridging Ligand 2,3-Bis(2-pyridyl)pyrazine (dpp)

M. Shoup, B. Hall, and R. R. Ruminski*

Received June 29, 1987

Recent investigations have used the bidentate nitrogen aromatic heterocyclic ligands 2,3-bis(2-pyridyl)pyrazine (dpp),[1,2] 2,2′-bipyrimidine (bpym),[3-5] and 2,3-bis(2-pyridyl)quinoxaline (dpq)[6] in the preparation of mono- and bimetallic Ru(II) polyazine complexes. Interest in $Ru(L)_3^{2+}$ (L = bpy, bpym, dpp, or dpq) arises from the fact that these complexes possess highly absorbing MLCT transitions in the visible spectrum, are photoinert, and undergo emission in fluid solution with lifetimes of several hundreds of nanoseconds.[1,2,4,6-8] These photophysical properties make such complexes ideal in bimolecular photocatalyzed water-splitting or energy-transfer processes.[8-15] Polymetallic intramolecular energy transfer has been explored as an alternative approach that bypasses the considerable difficulties associated with bimolecular energy transfer.[2] The polymetallic complex incorporates a highly absorbing, photoinert antenna fragment that can transfer energy through a bridging ligand, such as dpp or bpym, to a remote reactive metal fragment that does not absorb visible radiation.

Cr, Mo, and W carbonyl fragments bound to nitrogen aromatic bridging ligands have received some attention as antenna fragments in these polymetallic complexes.[16] An advantage of metal carbonyl antenna fragments is the negative solvatochromism of the MLCT transition in a wide variety of solvents.[16-22] With use of only differential solvents, the energy of the MLCT state of the antenna fragment could potentially be tuned to probe or exploit the acceptor levels of the reactive fragment.

Our research group has been involved in the preparation and characterization of potential antenna complexes containing the bridging ligands bpym or dpp.[23] We wish to report the prepa-

(1) Braunstein, C. H.; Baker, A. D.; Strekas, T. C.; Gafney, H. D. *Inorg. Chem.* **1984**, *23*, 857.
(2) Brewer, K. J.; Murphy, R. W., Jr.; Spurlin, S. R.; Petersen, J. D. *Inorg. Chem.* **1986**, *25*, 883.
(3) Dose, E. V.; Wilson, L. J. *Inorg. Chem.* **1978**, *17*, 2660.
(4) Hunziker, M.; Ludi, A. *J. Am. Chem. Soc.* **1977**, *99*, 7370.
(5) Ruminski, R. R.; Petersen, J. D. *Inorg. Chem.* **1982**, *21*, 3706.
(6) Rillema, D. P.; Taghdiri, D. G.; Jones, D. S.; Keller, C. D.; Worl, L. A.; Meyer, T. J.; Levy, H. A. *Inorg. Chem.* **1987**, *26*, 578.
(7) Navon, G.; sutin, N. *Inorg. Chem.* **1974**, *13*, 2159.
(8) Lin, C.-T.; Sutin, N. *J. Phys. Chem.* **1976**, *80*, 97.
(9) Balzani, V.; Moggi, L.; Manfrin, M. F.; Bolletta, F.; Laurence, G. A. *Coord. Chem. Rev.* **1975**, *15*, 321.
(10) Lin, C.-T.; Bottcher, W.; Chou, M.; Creutz, C.; Sutin, N. *J. Am. Chem. Soc.* **1976**, *98*, 6536.
(11) Kavarnos, G. J.; Turro, N. J. *Chem. Rev.* **1986**, *86*, 401.
(12) Dressick, W. J.; Meyer, T. J.; Durham, B.; Rillema, D. P. *Inorg. Chem.* **1982**, *21*, 3451.
(13) Bock, C. R.; Conner, J. A.; Gutierrez, A. R.; Meyer, T. J.; Whitten, D. G.; Sullivan, B. P.; Nagle, J. K. *J. Am. Chem. Soc.* **1979**, *101*, 4815.
(14) De Laive, P. J.; Sullivan, B. P.; Meyer, T. J.; Whitten, D. G. *J. Am. Chem. Soc.* **1979**, *101*, 4007.
(15) Rillema, D. P.; Allen, G.; Meyer, T. J.; Conrad, D. *Inorg. Chem.* **1983**, *22*, 1617.
(16) Moore, K. J.; Petersen, J. D. *Polyhedron* **1983**, *2*, 279.
(17) Lever, A. B. P. *Inorganic Electronic Spectroscopy*, 2nd ed.; Elsevier: Amsterdam, 1984.
(18) Kaim, W.; Kohlmann, S. *Inorg. Chem.* **1986**, *25*, 3306.
(19) Ernst, S.; Kaim, W. *J. Am. Chem. Soc.* **1986**, *108*, 3578.
(20) Ernst, S.; Kurth, Y.; Kaim, W. *J. Organomet. Chem.* **1986**, *302*, 211.
(21) Manuta, D. M.; Lees, A. J. *Inorg. Chem.* **1983**, *22*, 3825.
(22) Overton, C.; Conner, J. A. *Polyhedron* **1982**, *1*, 53.
(23) (a) Ruminski, R.; Johnson, J. *Inorg. Chem.* **1987**, *26*, 210. (b) Ruminski, R.; Wallace, I. *Polyhedron* **1987**, *6*(8), 1673. (c) Hiskey, M. A.; Ruminski, R. *Inorg. Chim. Acta* **1986**, *112*, 189. (d) Ruminski, R.; Van Tassel, K. D.; Petersen, J. D. *Inorg. Chem.* **1984**, *23*, 4380. (e) Ruminski, R.; Petersen, J. D. *Inorg. Chim. Acta* **1985**, *97*, 129. (f) Ruminski, R. *Inorg. Chim. Acta* **1985**, *103*, 159.

0020-1669/88/1327-0200$01.50/0